NASA-CR-201489

FINAL
IN-40
0017

Biospheric Effects of Volatiles Produced by the Chicxulub Cretaceous/Tertiary Impact

Final Report for National Aeronautics and Space Administration Contract NASW-4812

Kevin O. Pope

Geo Eco Arc Research

2222 Foothill Blvd., Suite E-272, La Canada, Ca 91011

14 June 1996

Preface

The evolution of life on Earth has been punctuated by numerous biological crises. Analyses of global, synoptic paleontological data bases of the last 500 million years identify five major, mass extinctions when a large percentage of Earth's species went extinct over a very brief period of time (e.g. Raup and Sepkoski 1982, 1986; Sepkoski 1990). These crises mark major shifts in evolutionary trends and play a critical role in the evolutionary process. Although recent advances have greatly improved our knowledge of the chronology, scale, and structure of mass extinctions, causes remains poorly understood. Any model of the evolution of life must account for this punctuated rhythm, and therefore studies of the causes of mass extinctions are needed.

The best studied cause of a major biological crises is the one proposed by Alvarez et al. (1980), who hypothesized that the dust cloud from an asteroid or comet impact caused the mass extinction that marks the end of the Cretaceous Period. The decade of research following the presentation of the Alvarez hypothesis produced substantial support (e.g. Alvarez and Asaro 1990). The recent recognition that the Chicxulub crater in the Yucatan Peninsula of Mexico is the site of the K/T impact (e.g. Hildebrand et al. 1991; Pope et al. 1991, 1993; Sharpton et al. 1992, 1993; Swisher et al. 1992) has provided the final confirmation that a major impact, perhaps the largest in the Phanerozoic, occurred at the K/T boundary.

While the impact portion of the Alvarez hypothesis is now widely accepted, the second part, that of a causal link between the impact and mass extinctions, remains controversial and in need of rigorous testing. The controversy is not surprising, given the inherent complexities of biological systems and their response to external forces (Jablonski 1994). Furthermore, previous studies of the K/T extinctions were impeded by a lack of constraints on the nature of the impact, which led to a seemingly endless list of possible extinction mechanisms. The discovery of the Chicxulub crater provides an ideal opportunity to constrain these possible mechanisms. In 1992 we began such a study of extinction mechanisms with support from the NASA Exobiology Program. Our project is an interdisciplinary one that combines studies of the crater geology with models of impact and atmospheric dynamics. We have focussed the study on the biospheric effects of volatiles, primarily sulfur gases, released by the impact into carbonate and evaporite terrain.

Introduction

The original hypothesis linking a large asteroid impact to the mass extinction recorded at the Cretaceous/Tertiary (K/T) boundary focussed upon the biospheric effects of silicate dust injected into the stratosphere (Alvarez et al., 1980). Subsequent modeling of this impact-generated dust cloud clearly demonstrated the potential of large impacts to block photosynthesis and cause global cooling, but also demonstrated that major effects would be transient, probably lasting no more than a few months and certainly less than 1 yr (Toon et al., 1982, 1994; Pollack et al., 1983; Covey et al., 1990, 1994). Other studies of possible K/T impact extinction mechanisms focussed on the potential of prolonged greenhouse warming caused by the stratospheric injection of water from an oceanic impact (Emiliani et al., 1981) or of CO_2 from an impact in carbonate terrain (O'Keefe and Ahrens, 1989). These two studies emphasized the importance of the volatile content of the impact site and the potential for volatiles to perturb the atmosphere and climate for years, rather than the months attributed to the dust.

Such extinction mechanisms, based as they were on unknown characteristics of the impact site, remained largely hypothetical until the Chicxulub crater in the northern Yucatan Peninsula of Mexico was identified as the K/T impact (Hildebrand et al., 1991; Pope et al., 1991). This discovery greatly intensified interest in volatiles because now the impact site is known to have contained large amounts of water, carbonate, and sulfate (e.g. Lopez Ramos 1979; Weidie 1985; Ward et al., 1995). The potential for the impact vaporization of sulfate rocks at Chicxulub presented a new possible extinction scenario, that of impact-generated sulfuric acid aerosols causing a lethal episode of global cooling and acid rain (Sigurdsson et al., 1991, 1992; Brett, 1992).

In this paper we expand upon our previous findings that these impact-generated sulfate aerosols produced about a decade of severe global cooling (Pope et al. 1994). We evaluate current knowledge of: 1) the energy of the impact; 2) the volatile content of the target rocks; and 3) shock pressures required to vaporize sulfates and carbonates. We revise our estimates of the mass of sulfur vaporized and include estimates of atmospheric injections of CO_2 and water vapor. Our atmospheric model has been improved to explicitly examine the role of water and to treat changing diffusion and aerosol production rates over time. These revisions and improvements strengthen our conclusion that impact-generated sulfate aerosols played a major role in the K/T mass extinction. We do not suggest that the sulfate cooling was the only extinction mechanism, nor do we imply that it was necessarily the major one, for several potential extinction mechanisms have been identified (e.g. Toon et al. 1994). We do propose that global cooling caused by sulfate aerosols is the only plausible long-term (several years) extinction mechanism known, as our research demonstrates that any long-term greenhouse warming produced by the K/T impact was insignificant by comparison.

Characteristics of the Impact Site

Composition

Recent studies of drill cores from the rim of the Chicxulub crater indicate that the approximately 3 km thick sequence of sediments present at the time of impact was composed of 35-40% dolomite, 25-30% limestone, 25-30% anhydrite, and 3-4% sandstone and shale (Ward et al., 1995). These estimates are considered more accurate than previous ones based on well cuttings (e.g. Lopez Ramos, 1979), which placed the anhydrite volume near 60%. This discrepancy may result from contamination of the cuttings by anhydrite fragments from the overlying ejecta blanket, which contains abundant small chips of anhydrite (Ward et al., 1995). For this study we assume 70% carbonate (limestone and dolomite) and 30% anhydrite, with other lithologies being negligible.

Porosity and Surface Water

Porosity is well developed in carbonate platform sequences and we estimate a mean carbonate porosity of 20% at Chicxulub. This estimate is based on the published range of 14-26% for subsurface Late Cretaceous carbonates in the southwestern edge of the Yucatan platform (Viniegra-O., 1981), and on a range of 40% to 13% for the corresponding depths of 0-3000 m in a similar platform sequence in Florida (Schmoker and Halley, 1982). This estimate is conservative, since as the Florida data show, the upper several hundred meters of carbonate probably had porosities much higher than 20%. Anhydrites by contrast have little to no porosity. The Yucatan platform was mostly submerged at the time of impact, hence all pore spaces would have been filled with sea water.

The upper-most Cretaceous beds overlain by ejecta near the crater rim are shallow water carbonates, and in the Yucatan 2 well they include evaporites (Weidie, 1985; Ward et al. 1995). Nevertheless, a precise record of the depositional environment at the time of impact is missing since the emplacement of the ejecta probably eroded many meters of latest Cretaceous sediment. For example, no Maastrichtian sediments have been identified beneath the ejecta on the crater rim, although late Maastrichtian foraminifera are found in the mud matrix of the ejecta (Ward et al., 1995), probably derived from ejecta scouring of unconsolidated sediments on the rim.

The Late Cretaceous sequence at Chicxulub, especially the return to evaporite deposition in the Yucatan 2 well, indicates a lowering of sea level prior to impact. This trend is noted throughout much of the Gulf of Mexico following the middle Maastrichtian transgression (Sohl et al., 1991) and may have been global (Haq et al., 1987). Many of the sedimentary sequences in the southern Gulf of Mexico have evidence for marked erosion at the K/T boundary, but their is considerable controversy as to whether the erosion was caused by the Chicxulub impact or a by a marine regression (e.g. Alvarez et al. 1992; Smit et al. 1992, 1994; Keller et al. 1993; Stinnesbeck et al. 1993, 1994). While there is little doubt that the impact disrupted sedimentation throughout Gulf of Mexico, it is also probable that there was a sea level low stand at the time of impact.

We conclude that while water depths at the time of impact remain uncertain, the limited core data combined with sea level trends within the Gulf of Mexico suggest that water depths were minimal. We assume no appreciable open water existed at the time of impact. Since a large amount of water was present as pore water in the carbonates (equivalent to ~420 m depth), a few tens of meters of surface water, if present, would be negligible in our impact calculations.

Impact Vaporization of Carbonates, Sulfates and Water at Chicxulub

Previous experimental and theoretical research on carbonates suggests that vaporization occurs between 10-70 GPa (e.g. Kieffer and Simonds, 1980; Boslough et al., 1982; Lange and Ahrens, 1986; Tyburczy and Ahrens, 1986; O'Keefe and Ahrens 1989). Such a large spread in values reflects both the dependence of vaporization experiments on pCO_2 and sample porosity, as well as difficulties in linking theoretical and experimental results. Two of the most recent calculations found nearly identical values for incipient vaporization of crystalline calcite, 56±6 GPa (Yang et al., 1996) and 56 GPa (Badjukov et al. 1995), and for complete vaporization of crystalline calcite 103±12 GPa (Yang et al. 1996) and 111 GPa (Badjukov et al. 1995). Studies of shocked limestones and dolomites in the Haughton crater found evidence of vaporization (decarbonization) only in rocks shocked >50 GPa (Martinez et al., 1994). Both Martinez et al. (1995) and Badjukov et al. (1995) conducted shock experiments and found no appreciable vaporization of crystalline dolomite or calcite at pressures up to 60 GPa. Given these recent results, previous estimates of the amount of CO_2 released in large impacts (e.g. O'Keefe and Ahrens, 1989), including our own for Chicxulub (Pope et al., 1994), need to be revised downward.

Yang et al. (1996) and Badjukov et al. (1995) also present nearly identical calculations for the vaporization of crystalline anhydrite, with incipient vaporization at 81$\pm$7 GPa and 80 GPa for the two research groups respectively, and complete vaporization at 155$\pm$13 GPa and 162 GPa respectively. These results are also similar to those of Chen et al. (1994) and the upper value (100 GPa) used in our previous study (Pope et al., 1994).

In this study, we adopt values of 70 GPa for the complete vaporization of carbonate and 100 GPa for the complete vaporization of anhydrite. For water, we adopt a vaporization pressure of 10 GPa, based on the calculations of Kieffer for the impact vaporization of water contained within rock pore space (Kieffer and Simonds, 1980; Alvarez et al., 1995).

The maximum theoretical values for crystalline calcite and anhydrite are not used because the experimental and theoretical studies noted above clearly show that porous materials and mixed lithologies vaporize at lower pressures than pure crystals. For example, Martinez et al. (1995) suggest that an increase in porosity from 0% to 4% can lower vaporization pressures 10 GPa in calcite and dolomite. Badjukov et al. (1995) calculate that when calcite is mixed with quartz, incipient and complete vaporization pressures drop to about 32 GPa and 48 GPa respectively. The same study also demonstrates that when anhydrite is mixed with quartz incipient and complete vaporization pressures drop to about 31 GPa and 80 GPa respectively. Our estimates are therefore conservative, although it is difficult to predict the effects of porosity and target heterogeneity on scales of tens to hundreds of meters found at Chicxulub, compared to microns to millimeters tested in the laboratory.

Energy of the Chicxulub Impact

The energy of the Chicxulub impact is related to the mass and velocity of the impacting body, which are two of the parameters we use in our impact models. Five main sets of parameters have been used to estimate the energy of the impact: 1) crater size; 2) ejecta volume (thickness); melt sheet volume and chemistry; 4) meteoritic content in the global ejecta; and 5) population and size statistics of asteroids and comets that cross the Earth's orbit (Earth-crossing). Each of these are briefly evaluated below.

Crater Size

The final crater diameter (D_f) is not related to impact energy in a straightforward way and most researchers scale impact energy with the transient crater diameter (D_{tc} = diameter of the bowl shaped cavity that forms immediately after impact prior to collapse of the rim and rebound of the crater floor). Our knowledge of the relationship between D_{tc} and impact energy is also very imprecise (Melosh, 1989:121), but determination of the D_{tc} of the Chicxulub crater remains one of the best methods for estimating the energy of the impact.

Much of the controversy and confusion about the size of the Chicxulub crater centers around defining D_f and D_{tc}. Since the transient crater is by definition transient, it cannot be measured directly and is instead inferred from other structural elements (central uplift, peak ring, terrace zone, etc...) and theoretical calculations (e.g. Grieve et al., 1981; Croft, 1985). Furthermore, since the crater is buried, neither D_f nor the structural features used to define D_{tc} can be directly measured.

Our recent analysis of the surface expression of Chicxulub suggests that much of the buried crater morphology is reflected in subtle topographic features. We interpret Chicxulub as a peak ring structure, where a concentric topographic ridge at with a radius of 129±5 km corresponds with the buried crater rim indicating a D_f of ~260 km (Pope et al. in press). This diameter is slightly larger than the D_f of 240 km we proposed earlier based on scaling from the inferred crater floor and limited coring (Pope et al. 1993). We identified a surface trough feature at a radius of 62±5 km that may correlate with a ring fault marking the inner-most terrace. A roughly concentric topographic ridge, which we interpret as the surface expression of the buried peak ring (radius ~52 km), lies between the previously mentioned outer trough and another inner trough at 41±2. Croft's (1985) analysis of large complex craters places the transient crater rim just within the inner-most terrace and outside of the peak ring. Using our topographic analysis and Croft's criteria we infer a D_{tc} for Chicxulub of ~124 km (diameter of the outer trough), which agrees well with a D_{tc} of 125 km predicted by Croft's power function scaling of a 260 km diameter terrestrial crater formed in sedimentary rocks.

Hildebrand and colleagues (Hildebrand et al., 1991, 1995; Pilkington et al. 1994) argue for a Chicxulub D_f of 180 km and a D_{tc} of 80-90 km, based on the analysis of gravity and magnetic data and hydrological features. Espindola et al. (1995) suggest a D_f of about 200 km based on the analysis of gravity and magnetic data and although they do not estimate D_{tc}, they do interpret Chicxulub as a peak ring crater with a ring radius of ~52 km (measured from their data using our [Pope et al. in press] estimate of the crater center).

In contrast, Sharpton et al. (1993, in press) analyzed gravity and core data from which they inferred a D_f of 260-300 km and a minimum D_{tc} of 120 km and a possible D_{tc} of 145-195 km.

We find some convergence between the work of Sharpton et al. and our own. This is especially true if Sharpton et al.'s minimum values for D_f and D_{tc} are considered. Their larger values may be too large, but certainly set an upper limit. There is also agreement between Sharpton et al. (1993), Espindola et al. (1995), and Pope et al. (in press) on the location of the peak ring at a radius of ~52 km. The work of Hildebrand an his colleagues and Espindola et al. also appear to converge with respect to D_f, but we find several problems with their crater diameter estimates. We agree that the gravity data indicate a major structural feature lies at a diameter of 180-200 km, but we interpret this feature as a terrace scarp, not the final crater rim, because concentric topographic features (Pope et al., in press) and subtle gravity anomalies (Sharpton et al., 1993) extend well beyond this feature. In our opinion, and that of Sharpton et al. (in press) as well, it has never been conclusively demonstrated that the major gravity feature at Chicxulub must correlate with the final crater rim, and in fact this appears not to be the case for the ~ 90 km diameter Chesapeake Bay crater (Poag, 1996).

Hildebrand et al. (1995) equate the location of the transient crater rim with a gravity low that they interpret as the peak ring at a radius of 40-45 km. Such a position for the transient crater rim is at odds with the study of Croft (1985), who finds that the peak ring merely sets an inner bound for the transient crater rim. Furthermore, we (Pope et al. in press) find it more likely that the buried peak ring correlates with the aforementioned topographic ridge at a radius ~52 km, rather than a trough at ~41 km. Sharpton et al. (1993, in press) also find Hildebrand et al.'s (1995) placement of the peak ring at odds with their gravity analysis, which places the peak ring along a gravity high at a radius of ~ 52 km.

Ejecta Thickness

The relationship between crater diameter and ejecta thickness that was developed by McGetchin et al. (1973) was applied to the Chicxulub case by Kring (1995), who concluded that observed ejecta thicknesses support a D_f of 180 km. McGetchin et al. (1973) used the term "original crater excavation" not transient crater in their analysis, but it is clear from the application of their scaling relationship to the inner rings of complex craters that D_{tc} is the appropriate parameter for Chicxulub. Kring (1995), like Hildebrand and Stansberry (1992) and Vickery et al. (1992), mistakenly used D_f (180 km) not D_{tc} in their predictions of Chicxulub ejecta thickness. Hence if ejecta thicknesses scale well with a D_{tc} of 180, as these analyses seem to indicate, then ejecta thicknesses support the large D_f of 300 km proposed by Sharpton et al. (1993), which better corresponds to a D_{tc} of 180 km.

Nevertheless, if the possible range of D_{tc} values is considered for a given D_f (e.g. D_{tc} = 0.5-0.65D_f, Grieve et al., 1981), as well as the error margins in the McGetchin scaling, then there is considerable overlap between the predicted ejecta thicknesses for the 180 and 300 km diameter craters. Thus, the observed Chicxulub ejecta thickness do not provide for a definitive determination between the two crater diameters, although the best fit is for a D_{tc} of ~160 km (e.g. the McGetchin scaling for a D_{tc} of 160 km predicts ejecta thicknesses of 42 cm in Haiti and 3 cm in the Raton Basin, which compares well with the values reported in Kring [1995]). An important caveat, in part recognized by Kring (1995), is that the McGetchin et al. (1973) relationship was developed from explosion experiments and its validity for large craters has only been demonstrated for proximal ejecta 100s of m thick. Its application to the distribution of cm-thick distal ejecta deposits from a large impact crater is questionable and probably not very precise.

Impact Melt Volume and Chemistry

Another method used by Kring (1995) to estimate the energy of the impact is to relate melt volume to D_{tc}, from which he inferred a D_{tc} of 100 km. Kring's analysis is complicated by uncertainties derived from the D_r-D_{tc} relationship, as well as by the lack of data on the dimensions of the Chicxulub melt sheet. Nevertheless, Kring demonstrates that the very large D_{tc} values (e.g. 195 km) proposed by Sharpton et al. (1993, in press) convert to unlikely melt sheets thicknesses of tens of kilometers if the melt is confined to within the peak ring. We, too, find such thicknesses unlikely, however we must admit that there are no data to conclusively refute such estimates. Furthermore, given the large volatile content of the Chicxulub target, large volumes (90-99%) of melt may have been dispersed by expanding gases (Kieffer and Simonds, 1980). Current data on the melt sheet dimensions do not permit distinctions between less disparate melt volumes predicted for D_{tc}s of 124 km versus 100 km or 90 km.

Kring's (1995) analysis of the melt sheet geochemistry is similarly informative, but not conclusive. The absence of a mantel component in the samples analyzed is important to note, for had such material been found it would provide strong evidence for a large D_{tc}. The absence of evidence in this case is less compelling, since the handful of samples thus far analyzed come from near the surface of a melt sheet that must be at least several km thick. It is quite possible that these samples do not adequately represent the composition of the entire melt sheet. Nevertheless, we find the lack of a mantel component is consistent with the other evidence noted above in suggesting that the very large D_{tc} (e.g 195 km) proposed by Sharpton et al. may be too large.

Meteoritic Content of the K/T Boundary Layer and the Size of the K/T Impactor

The fourth method, based on derivations of the projectile mass, is the one originally applied by Alvarez et al. (1980) to estimate the magnitude of the K/T catastrophe. Alvarez and his colleagues used both the iridium (Ir) content and overall mass of the K/T boundary clay to calculate an asteroid mass between 3-32 x 10^{17} g (diameter of ~7-14 km). Many of the assumptions used in these early calculations have since been modified and many more measurements have been made of the extraterrestrial component in the K/T boundary clay. These refinements suggest a projectile mass of 4.5-9.8 x 10^{17} g (Kyte et al., 1985), which corresponds to a chondritic asteroid diameter of ~7-10 km.

Despite these refinements, considerable uncertainty remains in such estimates of the projectile mass. As Kyte et al. (1985) note, the meteoritic component in the K/T boundary clay has undergone significant fractionation and redistribution and the amount of meteoritic material varies considerably from site to site (e.g. Ir concentrations can vary by a factor of 40). Kyte et al.'s estimates are conservative, as they assume that only the meteoritic material in the basal layers of the boundary clay are primary fallout, with the rest of the material representing enrichment of the site by lateral transport. While this assumption is reasonable, the possibility remains that the upper layers of the boundary clay are partly or mostly primary material as well, then the projectile could have had 2-3 times the mass and a diameter up to ~14 km.

Other uncertainties, more difficult to asses, derive from the possibility that part of the projectile mass was lost to space during the impact. Calculations presented by Vickery and Melosh (1990) suggest that for a 14 km diameter asteroid impacting at 20 km/sec little of the asteroid mass may be lost, but for the same projectile impacting at 35 km/sec, 80% may be lost. Given such a high velocity impact, the Vickery and Melosh calculations indicate that a 14 km diameter asteroid may leave a meteoritic trace equivalent to that of a lower velocity (20 km/sec) 8 km diameter asteroid. Hence, if Chicxulub were formed by a ~35 km/sec impact, the conservative estimates of meteoritic material by Kyte et al. (1985) are most consistent with an asteroid 14-20 km in diameter.

Earth-Crossing Comets and Asteroids

The most significant unknown in estimating the energy of the impact from estimates of the projectile mass is the velocity. Especially critical is the issue of whether the projectile was an asteroid or a comet, the latter of which can have 2-3 times the velocity, albeit 3/4 to 2/3 the mass for a similar-sized object. The calculations of projectile mass noted above were for asteroids. If the projectile were a comet, then the size estimates based on the meteoritic content of the boundary clay would be proportionately larger, how much so depending upon the water content of the comet. Sigurdsson et al. (1992) calculate that the global Ir mass found at the K/T boundary could only be deposited by a comet impact given the size limitations imposed on the impactor by the ~180 km D_f of the Chicxulub crater. These calculations, however, misinterpreted the crater-projectile scaling relationship of Schmidt and Housen (1987) presented in Vickery and Melosh (1990), which related D_{tc}, not D_f, to projectile size. The possible range of D_{tc}s for Chicxulub, as discussed above, coupled with the range of possible Ir masses, can accommodate either an asteroid or comet impact.

Shoemaker et al. (1990) demonstrate that a 10 km diameter comet impacting Earth is more than three times more likely to occur than is the impact of a 10 km diameter asteroid. Their calculations predict 1 such comet impact in the last 100 million years, and no such asteroid impact. No >10 km diameter asteroids are known to cross the Earth's orbit (Aten or Apollo class), although a few Amor class asteroids have diameters >10 km and orbits that could, over time, change and cross the Earth's orbit. There are an estimated 20 Earth-crossing asteroids with diameters > 5 km, two of which, 3200 Phaethon (6.9 km diameter, ~35 km/sec) and 1580 Betulia (7.4 km diameter, 30.6 km/sec) (Rabinowitz et al. 1994), have approximately enough kinetic energy to form a ~180 km diameter crater on Earth.

In overview, a comet impact is slightly more probable than an asteroid impact, but given that impacts such as Chicxulub are exceedingly rare to begin with, such statistics must be put in the context of rare events. Clearly both comets and asteroids must be considered as possible projectiles. The size of the transient crater, coupled with the amount of meteoritic material in the K/T boundary layer, place bounds on the probable size and velocity of the projectile. We find that the best estimates for the D_f and D_{tc} of Chicxulub are 260 km and 124 km respectively, but that these findings are not conclusive. We suggest that D_{tc}s <110 km and >165 km are unlikely for Chicxulub. If we combine the 450-980 Gt estimates of the projectile mass from Kyte et al. (1985) with the percent projectile mass lost to space (Vickery and Melosh, 1990) for the possible range of crater sizes using the Schmidt and Housen (1987) scaling relationship, we can calculate the range of possible Chicxulub projectile sizes. The range of possible asteroid (density 2-3 g/cm^3) diameters is 9.4-16.8 km, and for short period comets (density 1.5-2 g/cm^3) 14.2-24.0 km. No reasonable size or density of long period comet (velocity >40 km/sec) can be accommodated.

Volatile Mass Produced from the Sedimentary Layer at Chicxulub

Our estimates of the mass of volatiles injected into the atmosphere by the Chicxulub impact are based on our earlier 2-D hydrocode model of the Chicxulub impact (Pope et al., 1994; Ivanov et al., in press). This model provides estimates of the volumes of Mesozoic sediment shocked to within specific pressure ranges. Ivanov et al. (in press) modeled a range of projectile diameters and velocities (Table 1), which bound our estimates of the possible impact energies. Given the discussion in the previous section, the most likely configuration modeled by Ivanov et al. (in press) is that of a 14 km diameter, 38 km/sec

Table 1. Target volatile mass injected into atmosphere.

Crater Diameter (D_f) km	Projectile Diameter km	Projectile Velocity km/s	*SO_2 Gt (10^{15} g) F.	*SO_2 O.F.	*SO_2 Total	#CO_2 Gt (10^{15} g) F.	#CO_2 O.F.	#CO_2 Total	^H_2O Gt (10^{15} g) F.	^H_2O O.F.	^H_2O Total
180	10	20	98	16	114	159	48	207	32	280	312
220	12	25	140			234			48		
300	14	38	192	65	257	317	207	524	70	400	470
300	16	30	247			416			84		
300	18	25	313			527			107		
300	20	20	384	33	417	648	97	745	133	400	533
300	22	25	467			787			160		
300	24	25	556			936			190		

*based on 3 km thick section with 30% anhydrite @ 2.9 g/cm^3 shocked 100 GPa.
#based on 3 km thick section with 70% carbonate with 20% porosity @ 2.8 g/cm^3 shocked 70 GPa.
^based on water in 20% porosity in 2.1 km thick carbonate section @ 1.0 g/cm^3 shocked 10 GPa.
F. = vapors from footprint
O.F. = vapors from out-of-footprint
Note: Hydrocode model grid size prevented accurate calculations of O.F. water vapor mass for craters >180 km. The 400 Gt estimates are extrapolations of the calculations provided by Ivanov et al. (in press).

asteroid. The hydrocode model is not yet adapted to cometary or oblique impacts and our specific results pertain to only vertical asteroid impacts. While cometary impacts are not explicitly treated, our comparison of the effects of "small-fast" versus "large-slow" asteroids does capture some of the variability expected from cometary versus asteroidal impacts.

The volumes of sediments shocked to specific pressure ranges, when coupled with our estimates of target composition and vaporization thresholds presented above, allow us to calculate volatile masses (Table 1). These masses are calculated for two domains: the footprint, corresponding to the region immediately beneath the projectile; and the out-of-footprint, corresponding to the region of shocked sediments outside the direct path of the projectile (Figure 1). Given the simple geometry of our impact model, we can extend Ivanov et al.'s (in press) results to cover the full range of possible projectile diameters for the footprint volatile mass derived from the 3 km-thick sediment layer (Table 1), if we assume that all rock within the footprint is vaporized (valid for impacts >20 km/sec).

The importance of the distinction between these two regions lies in the evolution of the vapors. The footprint material first travels down into the transient crater, where it is mixed with highly shocked silica-rich basement rocks, and is ejected with the hottest vapors many seconds after initial impact (Ivanov et al. in press). The out-of-footprint material begins to degas within 1-2 seconds after impact and is ejected in a less hot part of the vapor plume. Alvarez et al. (1995) refer to these two portions of the plume as the "hot fireball" (footprint) and "warm fireball" (out-of-footprint).

The volatile mass estimates in Table 1 are conservative, as they do not include any volatiles from the vaporized projectile, nor do they consider the larger volume of vaporized

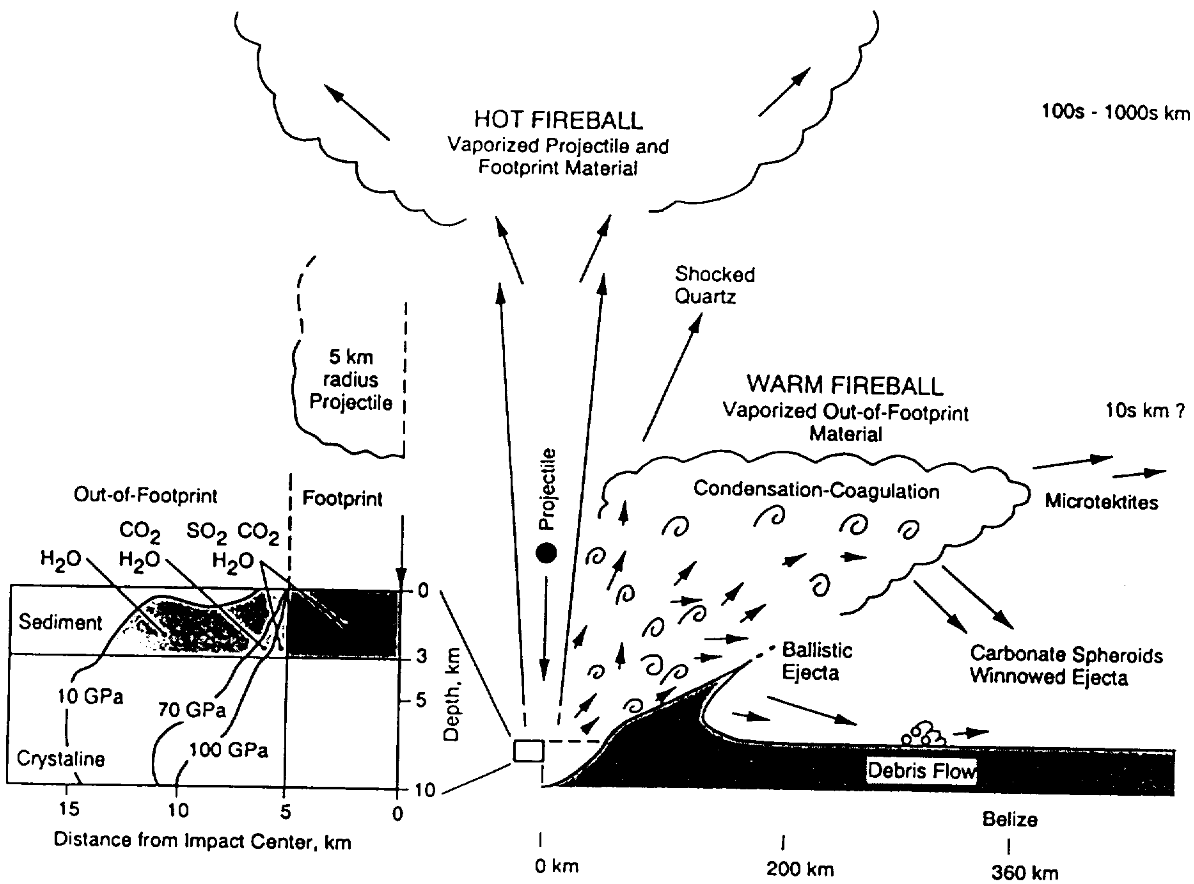

Figure 1. Model of vapor plume evolution. Left side diagram shows results of 2-D hydrocode model (left half only of symetrical model) of a vertical impact of a 10 km diameter, 20 km/sec, asteroid into a wet sedimentary layered target (adapted from Pope et al., 1994). Shown are the footprint and out-of-footprint regions with shock pressures (in GPa) and respective volatile species that are released. The right side of the diagram presents a schematic view of the origin and tragectories of the hot and warm fireballs that evolve from the footprint and out-of-footprint regions respectively. The hot fireball blows out of the upper atmosphere and is distributed globally (in high velocity impacts some material is ejected out of Earth orbit). Part of the warm fireball may also blow out of the upper atmosphere and spread globally, but a portion expands latterally, passing through the ejecta curtain, altering the trajectories of the finer ejecta. This latteral blast slows and cools rapidly, depositing particles that condense and coagulate in the plume: a possible origin of the carbonate spherules found in Belize (Ocampo et al., in press).

rock produced by an oblique impact. These factors are briefly addressed in the next section.

Evolution of the Vapor Plume

Warm Fireball

The vapors in the warm fireball are dominated by H_2O, with small amounts of CO_2 and SO_2 (Table 1) and do not contain much silicate vapor. The total mass of the warm fireball for a 10 km diameter, 20 km/sec vertical asteroid impact at Chicxulub is about 250 Gt, and for a 14 km diameter, 38 km/sec impact it is >500 Gt (Table 1). A 500 Gt fireball composed of the gases listed in Table 1 converts to about 400,000 km^3 of gas at standard temperature and pressure. Much of this mass would expand into the stratosphere, but perhaps only on a regional basis.

The warm fireball probably condenses much more rapidly than the hot fireball given its lower initial temperature. Given the moderate to low vaporization temperatures of carbonates and water, the temperature of the warm fireball may not exceed 2000° K. Rapid expansion of the vapors may also result in much of the gas not reaching thermodynamic equilibrium. Under these conditions of moderate temperatures and rapid expansion, some of the vaporized sulfates may evolve as SO_3, not SO_2, as indicated by thermodynamic models (Lyons and Ahrens, 1996) and by laser vaporization experiments (Gerasimov et al., 1994, 1995; Ivanov et al., in press).

The initial expansion of the warm fireball would occur in direct contact with rock fragments of the ejecta curtain (e.g. Alvarez et al., 1995; Ocampo et al., in press). The warm fireball would be highly turbulent where it interacted with the ejecta and atmosphere. Presumably some mixing with the hot fireball would occur, but being as the hot fireball develops several seconds later, the warm fireball could expand 100 km prior to the initial expansion of the hot fireball.

Hot Fireball

The hot fireball is comparable to the K/T vapor plume modeled by several investigators (e.g. Vickery and Melosh, 1990; Zahnle 1990), and is somewhat similar to the fireball modeled for the Shoemaker-Levy 9 comet impact of Jupiter (e.g. Takata and Ahrens, 1995; Zahnle et al., 1995). These impact plume studies demonstrate that the vapors in the hot fireball rapidly blow out of the top of the atmosphere and spread, in the K/T case, around the Earth. The hot fireball contains large amounts of CO_2, SO_2, and lesser amounts of H_2O, derived from the Mesozoic sediments (Table 1). The hot fireball contains much l-arger amounts of vapor derived from the silicate basement rocks. Based on scaling relationships developed by O'Keefe and Ahrens (1982) and presented by Melosh (1989:122), the amount of vapor produced by a 14 km diameter, 38 km/sec vertical asteroid impact into a silicate target would be ~32,000 Gt. Given the high volatile content of the Yucatan target, a Chicxulub vertical impact would have produced slightly more. The CO_2, SO_2, and H_2O vapors in the hot fireball from such an impact would total only about 580 Gt (Table 1), or about 2% by weight.

A hydrodynamic model of the Shoemaker-Levy 9 impact indicate that a 2 km diameter comet impacting at 60 km/sec (~10^{29} ergs) would produce a hot fireball with initial temperatures >10,000° K and temperatures >2000° K >100 sec after impact (Takata and Ahrens, 1995). The Chicxulub impact had 100 times as much energy, therefore temperatures would probably exceed 3000° K for several minutes as the hot fireball expanded. Given these temperatures and time intervals, the vaporized sulfate would reach thermodynamic equilibrium and evolve as SO_2 (Lyons and Ahrens, 1996). The reentry of condensed vapors and melt from the hot fireball from a 10 km diameter asteroid impact at 20 km/sec would heat the upper stratosphere to about 800° K on a global scale (Zahnle 1990). The higher energies (~5-15 times) we suggest for Chicxulub would heat the stratosphere enough (~1000-1200° K) to vaporize any dolomite or calcite solid ejecta and any water in the upper stratosphere on a global scale (Zahnle, 1990). Stratospheric temperatures would also reach temperatures high enough (~1800° K) to vaporize sulfate solid ejecta over a large area, though perhaps not globally (cf. Zahnle, 1990). Such secondary heating of the stratosphere by ejecta upon reentry would prevent any early-stage condensation of these volatile species and therefore ensure global distribution of the SO_2, CO_2, and H_2O vapors.

Volatiles from the Projectile

Estimates of the CO_2, SO_2, and H_2O from the projectile are not included in Table 1. The composition of the projectile is unknown and therefore such estimates are purely speculative. Some plausible projectiles have very little sulfur, carbon, or water. Furthermore, the amount of meteoritic volatiles deposited in the stratosphere is not simply a function of the volatile content of the projectile. Recent impact models suggest that as little as 20% of a 10 km diameter asteroid is vaporized in a 20 km/sec impact (Pierazzo et al., 1996). Most of the projectile may be vaporized in high-velocity impacts, but as noted above such impacts can result in >80% loss of the projectile mass to space (Vickery and Melosh, 1990). The estimates of meteoritic material in the K/T boundary provided by Kyte et al. (1985) can be used to place bounds on the possible volatile contribution of the projectile. Such estimates are presented in Table 2. Projectile vapors would reside within the hot fireball. A range of values for the sulfur, carbon, and water content of the projectile are used representing the maximum and typical percentages for sulfur and carbon in asteroids and a typical range of water contents for comets. In extreme cases the sulfur content of the projectile can increase SO_2 production by ~100%, but a more typical value is a 30% increase. Similar increases occur for CO_2. Dramatic increases in the H_2O production occur for cometary impacts.

Oblique Impact

There are several important factors relating impact vapor plumes and impact angle, but a full discussion of these factors is beyond the scope of this paper. Many of the relevant issues are discussed by Schultz and Gault (1990). Here we consider only first order modifications to our estimates of volatile mass and provide a brief overview of oblique effects on the evolution of the vapor plume. Future work is needed on the atmospheric effects of the Chicxulub impact.

The most probable impact angle is 45°. Schultz (1994, 1995) has argued that the

Table 2. Meteoritic Volatile mass injected into atmosphere*.

Projectile Mass Retained Gt (10^{15} g)	SO_2 Gt (10^{15} g)		CO_2 Gt (10^{15} g)		H_2O Gt (10^{15} g)			
	Asteroid/Comet		Asteroid/Comet#		Asteroid		Comet	
	6% S	2% S	3% C	0.5% C	17% H_2O	1% H_2O	50% H_2O	25% H_2O
450	54	18	50	8	77	5	450	225
980	118	39	108	18	167	10	980	490

* Assumes all the meteoritic S and C in the retained mass are converted to SO_2 and CO_2 and that the water in comets is vaporized and retained in the same proportion as present in the projectile. S, C, and asteroid H_2O percentages based on non-volatile component and represent the maximum and typical values for asteroids and comets. Projectile masses are the minimum and maximum values from Kyte et al. (1985).

Maximum C in an asteroid is about 3%, which is also typical of a 50% ice comet. A typical asteroid has about 0.5% C. No maximum C value for comets is given.

Chicxulub impact was highly oblique, perhaps 20-30° from the horizontal. While such interpretations remain speculative, clearly such a possibility must be considered. Schultz and Gault (1990) have examined the relationship between target vaporization and impact angle. Their experimental work suggests that in oblique impacts between 45-15°, greater heating of the target occurs than in vertical impacts by a factor of $\cos^2$ due to frictional rather than shock heating. Nevertheless, there is some question as to the applicability of these relatively low velocity experiments ($\leq$6 km/sec) to actual asteroid or comet impacts (Melosh 1989:121), largely due to the greater coupling of energy at high velocities. Furthermore, it is not clear how this increase in frictional heating would be partitioned in the upper 3 km sedimentary layer and how much more sediment would be vaporized.

A simpler approach to estimating the effects of an oblique impact is to calculate the increase in the volume of sediments within the impact footprint. The volume of the footprint increases by a factor of 1/sin (vertical impact = 90°). All of the footprint material was vaporized in our vertical impact model runs for velocities $\geq$ 20 km/sec. Given that the sedimentary cover is much thinner than the projectile diameter it is reasonable to assume that the entire footprint in a $\geq$20 km/sec oblique impact is vaporized as well. Clearly 3-D modeling of the effects of oblique are needed to better understand the effects of oblique impacts, but before such studies are completed, the 1/sin factor provides a reasonable upper limit for the increase in the amount of vaporized sediment in the hot fireball. For the most likely impact angle 45°, an increase of 40% is indicated. For the 30° impact suggested by Schultz (1995), the volume of vaporized sediment would double.

Another important effect of an oblique impact, discussed by Schultz and Gault

(1990), is that while the volume of the vapor plume may be higher in oblique compared to vertical impacts, the energy content of the plume is less resulting in a cooler plume. Therefore, oblique impacts may produce more vapor, but much of this vapor may condense rapidly and not be globally distributed. This is especially true for sulfur oxides, which may condense as sulfate ($CaSO_4$ or H_2SO_4). This implies that highly oblique impacts may not greatly increase globally distributed CO_2, SO_2, and H_2O in the stratosphere compared to near-vertical impacts. Hence a ~50% increase over the target volatile masses in Table 1 may be the maximum expected for an oblique impact.

Baseline Volatile Masses

Given the range of volatile masses in Tables 1 and 2 and the potential increases in the target volatile mass due to oblique impact, the maximum and minimum values for SO_2, CO_2, and H_2O ejected into the stratosphere and distributed globally by the Chicxulub impact cover a wide range. If we assume: 1) a near-vertical impact, 2) the smallest possible projectile (~10 km diameter), 3) only the hot fireball is globally distributed, and 4) minimal amounts of S, C, and H_2O in the projectile, then the global production of SO_2 would be ~100 Gt, CO_2 ~160 Gt, and H_2O ~30 Gt. Conversely, if we assume: 1) an oblique impact (50% increase in target volatiles), 2) the largest possible projectile (24 km diameter), 3) the hot and warm fireball vapors are globally distributed (and all sulfur gas evolves as SO_2), and 4) the projectile was a sulfur, carbon, and water-rich short period comet, then the global production of SO_2 would be ~1000 Gt, CO_2 ~1700 Gt, and H_2O ~1700 Gt.

These minimum and maximum values are, however, highly improbable as they are based on the combination of several atypical projectile characteristics. We propose more probable baseline estimates of the globally distributed stratospheric volatiles in Table 3 by changing a few of the assumptions to more reasonable values. To be conservative, we selected parameters that produce volatile masses toward the low end of the range of reasonable values. We selected an asteroid and a comet with the mass and velocity required to create a crater in the 230-260 km diameter range. The size of these projectiles falls within the lower 1/3 of the range of possible values for either asteroids or comets. We assume an oblique impact that caused a slight, 10%, increase in the target volatile mass given in Table 1. We assume that 30% of the out-of-footprint (warm fireball) is globally distributed in the stratosphere (as SO_2, CO_2, and H_2O vapor) based on the laser experiments in Ivanov et al. (in press). Typical S, C, and H_2O contents were used to estimate the volatiles contributed by the projectile. It was necessary to use the maximum estimate (980 Gt) of meteoritic material in the K/T boundary clay (Kyte et al., 1985) for the asteroid parameters and the minimum estimate (450 Gt) for the comet parameters to produce acceptable values.

Modeling Atmospheric Effects of Chicxulub Impact

Our previous analysis (Pope et al., 1994) of the atmospheric effects of the injection of a large mass of vaporized sulfate into the stratosphere focussed on two scenarios: 1) the rapid production of sulfuric acid aerosols, primarily from the warm fireball, and 2) the

Table 3. Baseline volatile mass globally distributed in stratosphere*.

Projectile		SO_2				CO_2				H_2O			
Diameter	Velocity	Gt (10^{15} g)				Gt (10^{15} g)				Gt (10^{15} g)			
km	km/s	F.	O.F.	P.	Total	F.	O.F.	P.	Total	F.	O.F.	P.	Total
Baseline Asteroid#													
12	28	154	10	39	203	261	33	18	312	53	120	10	183
Baseline Comet^													
16	28	272	13	18	303	458	40	50	548	92	120	450	662

*based on calculations in Tables 1 and 2 with the modifications noted below.
F. = vapors from footprint, increased 10% due to oblique impact.
O.F. = vapors from out-of-footprint interpolated from calculations in Table 1, assumes only 30% globally distributed in stratosphere.
P. = vapors from projectile, based on retained mass of 980 Gt for asteroid and 450 Gt for comet.
# 2.5 g/cm^3, 2% S, 0.5% C, 1% H_2O
^ 1.5 g/cm^3, 2% S, 3% C, 50% H_2O

slow production of sulfuric acid aerosols involving the time-limiting photochemical oxidation of SO_2 from the hot fireball. Here, we briefly review scenario #1, but focus more directly on improving our model of scenario #2 by explicitly examining the role of water and by incorporating higher temporal resolution in our treatment of the oxidation and diffusion of SO_2. We also examine the potential for greenhouse warming, primarily from impact-generated CO_2, in more detail.

Atmospheric Model

Our atmospheric modeling contains three parts: 1) a radiative transfer model (Baines and Smith 1990, Baines and Hammel, 1994); 2) a microphysical model of particle coagulation and sedimentation adapted from Toon et al., (1982); and 3) a SO_2 to H_2SO_4 conversion and stratospheric diffusion model adapted from Pinto et al. (1989) and empirical data. Sulfate aerosols reflect effectively, blocking sunlight from the troposphere and surface. We calculated solar energy deposition within the stratosphere using the optical constants for sulfuric acid of Palmer and Williams (1975) and Mie-scattering radiative transfer codes appropriate for spherical sulfate particles (Hansen and Hovenier, 1974) within a vertically-inhomogeneous atmosphere (Baines and Smith 1990, Baines and Hammel, 1994). The results are estimates of solar transmission at the surface for a given set of particle size, number density, and imaginary index of refraction (function of impurities in the sulfuric acid aerosols).

For the microphysical model, we assume a coagulation time t_{cg} for particles to combine in pairs, doubling in mass and increasing by 26% in radius:

$$t_{cg} = (10^6)\,(500/(n^*\langle r\rangle))^2$$

where n is the aerosol particle density (#/cm^3), <r> is the particle radius in microns and t_{cg} is in seconds. In all model runs we assume an initial particle radius of 0.5 microns and a particle density of 1.83 g/cm^3 (aqueous solution with 75% sulfuric acid). For our scenario #1 model we begin with particles evenly distributed between 20 km and 30 km. For our scenario #2 model we assume that aerosol particles are continuously produced at the 30 km level. Trial model runs with smaller initial particle sizes and higher formation elevations did not greatly effect the results. The fall speed for the sulfuric acid particles is:

$$v_f = (\langle r\rangle/0.5) * 50 \text{ mbars/year}$$

We found that over a wide range of initial particle number densities the time required for the particles to fall to the base of the stratosphere (10 km) is about one year, give or take a month. Below 10 km we assume that the particles quickly rain out in tropospheric weather systems.

The conversion of SO_2 to H_2SO_4 is self-shielding, caused by SO_2 absorption in the Hartley bands between 0.21 and 0.39 microns, as well as by efficient UV extinction by the sulfuric acid aerosols. Thus, photolysis of oxygen, ozone, and NO_2 are all significantly reduced, curtailing the abundance of free oxygen and NO needed to produce the OH radicals required to convert SO_2 to sulfate aerosol. The conversion rate of stratospheric reservoir gases produced by the Chicxulub impact into sulfate aerosols can be estimated by extrapolating the model results of Pinto et al. (1989), originally developed for volcanic injections of SO_2.

The Pinto et al. model applies to SO_2 injections of between 0.01-0.1 Gt, and the 1-2 month conversion rates for the ~0.01 Gt injections agree well with the conversion rates observed for the El Chichon and Pinatubo volcanic eruptions. As in Pope et al. (1994), we fit a power law to the model output of Pinto et al. (1989) in the form of:

$$Lso_2 = 32.1\ (Mso_2)^{0.6255}$$

where Lso_2 is the time scale for conversion of SO_2 to sulfate aerosol, in months, and Mso_2 is the mass of SO_2 injected into the stratosphere, in Gt (Figure 2). This power law relationship is supported by analyses of the Toba volcanic eruption ~71,000 years ago, which is estimated to have injected about 6.6 Gt of SO_2 into the stratosphere (Rose and Chesner, 1990; Rampino and Self, 1992). Recent analyses of sulfate precipitation in Greenland ice cores resulting from the Toba eruption indicate that conversion of the SO_2 to sulfate aerosol and its subsequent rain-out took about 6 years (Zielinski et al., 1996). This agrees well with the 5.3 years predicted by the application of our conversion power law coupled with the processes of diffusion (see below) and coagulation and sedimentation (Figure 2).

Most of the SO_2 injected into the stratosphere by the relatively small, historic volcanic eruptions is converted to sulfate aerosol. Nevertheless, when large masses of the SO_2 are injected not all of it is converted because diffusion of SO_2 to the troposphere

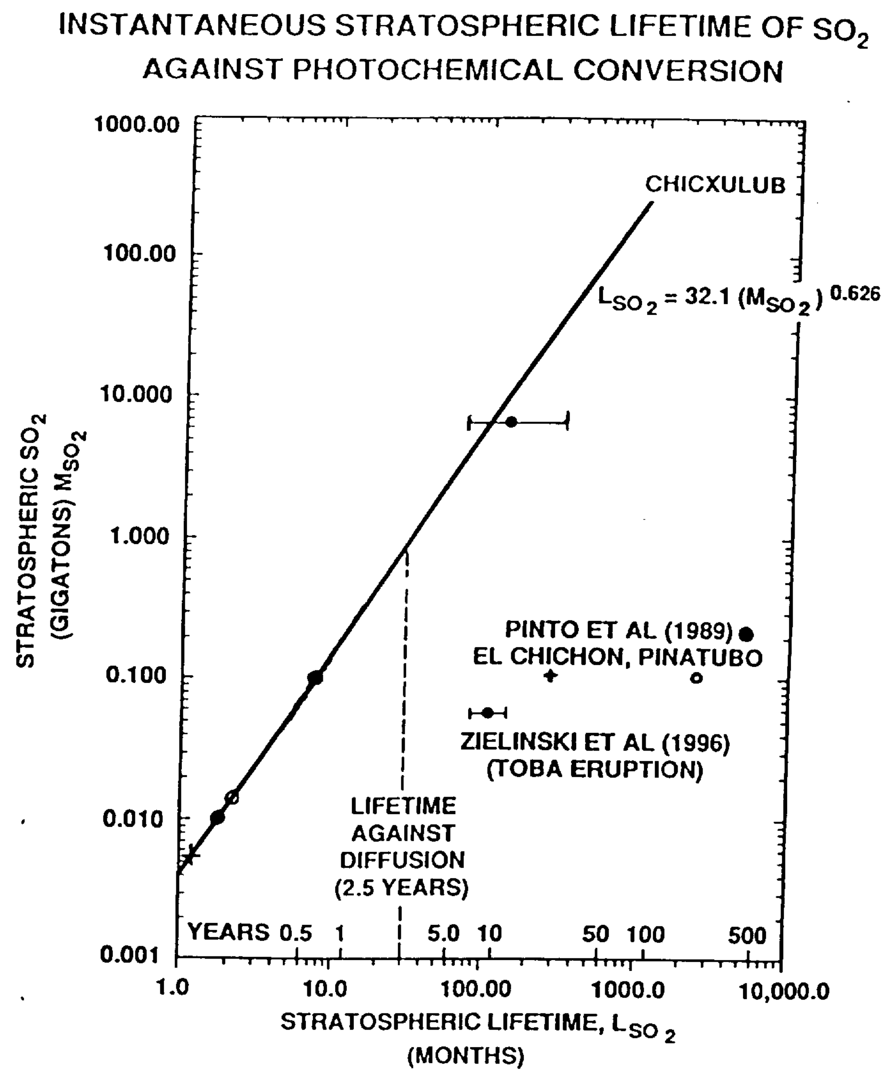

Figure 2. Instantaneous lifetime of stratospheric SO_2 (Lso_2) as a function of the initial mass loading of SO_2 (Mso_2). Power function based on a regression of lifetime values for 0.01 Gt (1.8 months) and 0.1 Gt (7.6 months) loadings calculated by Pinto et al. (1989). The Pinto et al. (1989) model agrees well with the observed limetimes for the El Chichon and Pinatubo volacanic eruptions. The power law extrapolation agrees well with the calculated lifetime (8.7 years) for the Toba eruption derived from the duration of sulfuric acid deposition recorded in the Greenland ice core (Zielinski et al., 1996). Lifetime (with error bars) for the Toba 6.6 Gt loading of SO_2 are calculated by inverting our model of coagulation and sedimentation to fit the 6±1.5 years of acid deposition noted by Zielinski et al. (1996).

occurs before conversion can take place. The time constant for stratospheric diffusion is ~2.5 years (Holton, 1990). Therefore, for SO_2 injections of >1 Gt, L_{SO_2} > 2.5 years, making the diffusion time scale the driver for the evolution of the stratospheric SO_2 reservoir. Again the Greenland ice core data for the Toba eruption provide a good check on our combined SO_2 conversion and diffusion model. Our model predicts that for a 6.6 Gt injection of SO_2, about 3.3 Gt of stratospheric H_2SO_4 should be produced, with the remain SO_2 diffusing to the troposphere. The Greenland ice cores indicate that 3.5 Gt of stratospheric H_2SO_4 was produced by the Toba eruption (Zielinski et al., 1996), in remarkable agreement with our model.

Figure 3 shows a schematic of the sulfate aerosol distribution within the stratosphere at the conclusion of the first year of the scenario #2 model (initial SO_2 reservoir = 200 Gt). For computational ease, the aerosol is divided into twelve layers, each associated with a mean monthly age. At the end of year 1, aerosols in the bottom layer rain out and a new aerosol mass is formed in the top layer using the SO_2 to H_2SO_4 conversion rate adjusted to the new SO_2 reservoir mass after depletion by acid conversion and diffusion. The sulfate mass is nearly constant in each layer, as the aerosol formation rate varies by only 15% during the year. In contrast, the aerosol particle number density decreases by nearly two orders of magnitude from top to bottom, reflecting the quadrupling of particle radius due to coagulation.

Sulfuric Acid Aerosols in the Warm Fireball: Scenario #1

Our discussion of the evolution of the warm fireball presented above emphasizes

STRATOSPHERIC IMPACT HAZE STRUCTURE FOR RADATIVE TRANSFER CALCULATIONS END OF YEAR #1

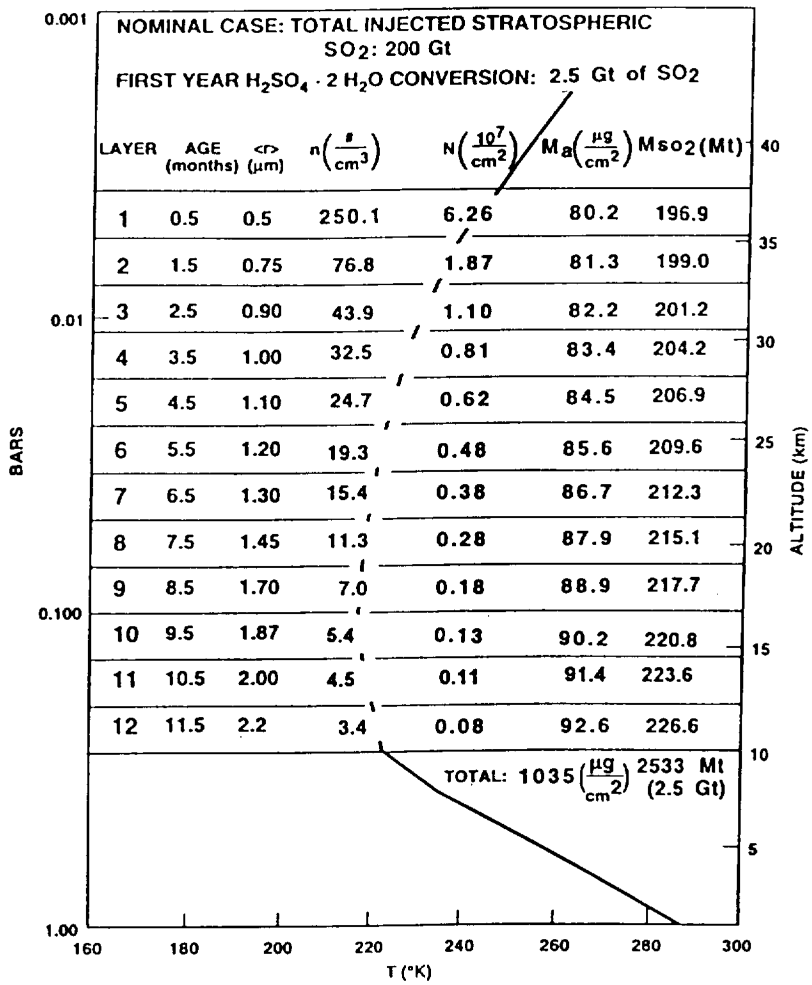

LAYER	AGE (months)	<r> (µm)	$n\left(\frac{\#}{cm^3}\right)$	$N\left(\frac{10^7}{cm^2}\right)$	$M_a\left(\frac{\mu g}{cm^2}\right)$	M_{SO_2}(Mt)
1	0.5	0.5	250.1	6.26	80.2	196.9
2	1.5	0.75	76.8	1.87	81.3	199.0
3	2.5	0.90	43.9	1.10	82.2	201.2
4	3.5	1.00	32.5	0.81	83.4	204.2
5	4.5	1.10	24.7	0.62	84.5	206.9
6	5.5	1.20	19.3	0.48	85.6	209.6
7	6.5	1.30	15.4	0.38	86.7	212.3
8	7.5	1.45	11.3	0.28	87.9	215.1
9	8.5	1.70	7.0	0.18	88.9	217.7
10	9.5	1.87	5.4	0.13	90.2	220.8
11	10.5	2.00	4.5	0.11	91.4	223.6
12	11.5	2.2	3.4	0.08	92.6	226.6
				TOTAL:	1035 $\left(\frac{\mu g}{cm^2}\right)$	2533 Mt (2.5 Gt)

Figure 3. Model structure of global stratospheric sulfuric acid aerosol haze one year after impact for nominal 200 Gt loading of SO_2. The haze is divided into 12 layers, spanning 10-30 km in altitude. The righthand altitude scale refers to the temperature profile (solid curve and bottom temperature scale), not to the physical location of the 12 layers. The precipitation time for sulfate aerosols formed at 30 km is one year, during which time the particles coagulate and grow into larger particles as thew fall. Each of the 12 layers shown pertains to a distinct mean aerosol age, in months. For each layer, values are listed for the mean number density (n), the layer column number (N) and aerosol mass (M_a) densities, and the mass of SO_2 within the layer (m_s in megatons, Mt). During the first post-impact month, 0.197 Gt of are converted to into stratospheric sulfate aerosol. Beginning with a mean particle radius of 0.5 microns, the particles grow to a radius of 2.2 microns as they fall into the troposphere. 2.5 Gt of sulfur are converted into sulfate aerosol during the first year.

the need to consider that a significant portion of the vaporized sulfates may rapidly combine with abundant water and form sulfuric acid aerosols either in the plume or soon after dispersal: our scenario #1. While we currently have no accurate means to calculate how much sulfuric acid could be rapidly produced, our baseline estimates, based on the laser experiments (Ivanov et al., in press), suggest that as much as 70% of the vaporized sulfur in the warm fireball may condense and rain out during the initial injection and dispersion in the atmosphere. This indicates that 20-30 Gt of SO_2 (or its S mass equivalent in SO_3 or SO_4) may convert to aerosol in the first few hours to days after impact. Much of this acid would probably rain out rapidly, but presumably a portion would be widely distributed, perhaps globally.

In Figure 4 we present our (Pope et al., 1994) microphysical and radiative transfer model of the radiative effects over time of

the rapid conversion of 10 Gt of SO_2 (5 Gt of S) into a globally distributed sulfuric acid aerosol cloud, which represents about half of the sulfur in our baseline warm fireball. These rapidly produced aerosols rain out in about 1 year, but initially cause severe disruption of solar transmission. Photosynthesis would be halted for about 1 month if the aerosols that formed were pure sulfuric acid solutions. This disruption of photosynthesis may have been extended to 6-9 months if the aerosols condensed on sub-micron silicate dust or soot particles, which would have also been injected along with the sulfate (Pope et al., 1994). Such particles greatly increase the absorption properties of the aerosols.

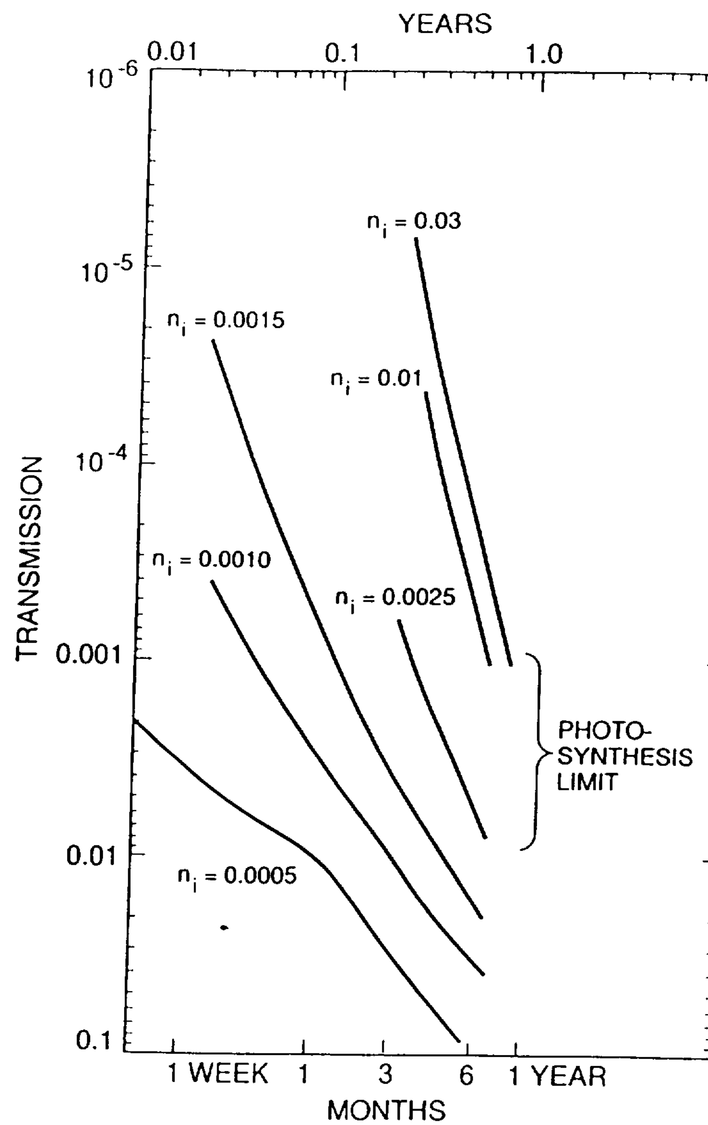

Figure 4. Reduction in solar transmission at the Earth's surface over time for an initial H_2SO_4 aerosol loading between 20 and 30 km of 5×10^{15} g of sulfur, which is equivalent to only about 5% of our sulfur mass estimates. Curves for different imaginary indices of refraction (n_i), which reflect possible impurities in the acid droplets. Soot $n_i = 0.03$; silicate dust $n_i = 0.0025$; pure H_2SO_4 aerosol $n_i = 0.0005$. Photosynthesis ceases when transmission drops below 0.001-0.01 (e.g. Toon et al. 1982). Once particles fall below 10 km we assume that they are removed immediately by meteorological processes.

Sulfuric Acid Aerosols in the Hot Fireball: Scenario #2

The major global atmospheric effects of the impact vaporized sulfates come from the long-term conversion of SO_2 and water vapor from the hot fireball into sulfuric acid aerosols. To create one molecule of H_2SO_4 from SO_2 and water one molecule of water must be destroyed: that which combines directly with the intermediate SO_3 via the reaction: $SO_3 + H_2O + M \rightarrow H_2SO_4$. The favored form of sulfuric acid aerosol in the Earth's stratosphere is $H_2SO_4 {*} 2H_2O$, hence a minimum of three water molecules are needed to produce sulfate aerosol from SO_2. Additional water may or may not be consumed in the formation of SO_3 from SO_2, which may occur through the consumption of 1/2 molecule of H_2O to produce an OH radical (Margitan, 1984), or through reaction with free O (e.g. Krasnopolsky and Parshev, 1983) consuming no water. Therefore, 3-3.5 water molecules are needed to produce sulfate aerosol from one molecule of SO_2, yielding an SO_2/H_2O mass ratio of 1.19-1.02.

Our baseline calculations indicate that the Chicxulub hot fireball produced a globally distributed stratospheric reservoir with 203-303 Gt of SO_2 and 183-662 Gt of H_2O vapor (Table 3). The current ambient stratospheric water mass is about 2.7-6.7 Gt (Houghton, 1977:165-166), however this amount is only about 1% of its saturated water vapor capacity due to the global cold trap of the tropopause that prevents tropospheric water from entering the stratosphere. Using the U.S. Standard Atmosphere, 1976 (e.g. Chamberlain, 1978:302) and the saturated vapor pressure over pure ice (e.g. Houghton, 1977:165-166), we find that the stratosphere could hold ~600 Gt of water vapor between 10 and 30 km altitude. Therefore, a direct injection of 183-662 Gt of water vapor into the stratosphere could be accommodated by ambient conditions. Furthermore, studies and models of volcanic SO_2 stratospheric injections demonstrates that such stratospheric loading heats the stratosphere several degrees (e.g. Labitzke et al., 1983; Brasseur and Granier, 1992), which would increase its saturated water vapor capacity. Such heating would likewise reduce cold trap effects due to latitudinal stratospheric temperature variations, which today tend to dry out the stratosphere. Thus the major sink for water and SO_2 was diffusion and conversion to aerosol. Given the 1.19-1.02 SO_2/H_2O mass ratio for such conversion, the impact would have produced sufficient stratospheric water to convert all or nearly all of the SO_2 to sulfate aerosol.

Figure 5 shows the evolution of our nominal impact-generated stratospheric reservoirs of SO_2 and H_2O, here taken to be 200 Gt each. This figure is derived from the coupling of the SO_2 conversion, diffusion, coagulation, and sedimentation components of our model. The major loss of stratospheric SO_2 and H_2O is from diffusion up until the last few years. Beginning the 12th year after the impact, the SO_2 and H_2O reservoirs are depleted to the point in which sulfate production is shut down within a few months. If the SO_2 and/or H_2O reservoirs were only 100 Gt, this would shorten the life of the sulfate clouds about 1.5 years, but still produce major effects for over a decade. Conversely, if the SO_2 and H_2O reservoirs were 300 Gt each, this would extend the effects about 1 yr, and if the reservoirs were 600 Gt each, the effects would be extended about 3 yrs (total ~15 years).

Applying our radiative transfer model we find that the stratospheric sulfate aerosols reflect back into space about 80% of the incident solar energy during the first year

EVOLUTION OF STRATOSPHERIC SO_2 AND H_2O IMPACT-GENERATED RESERVOIRS

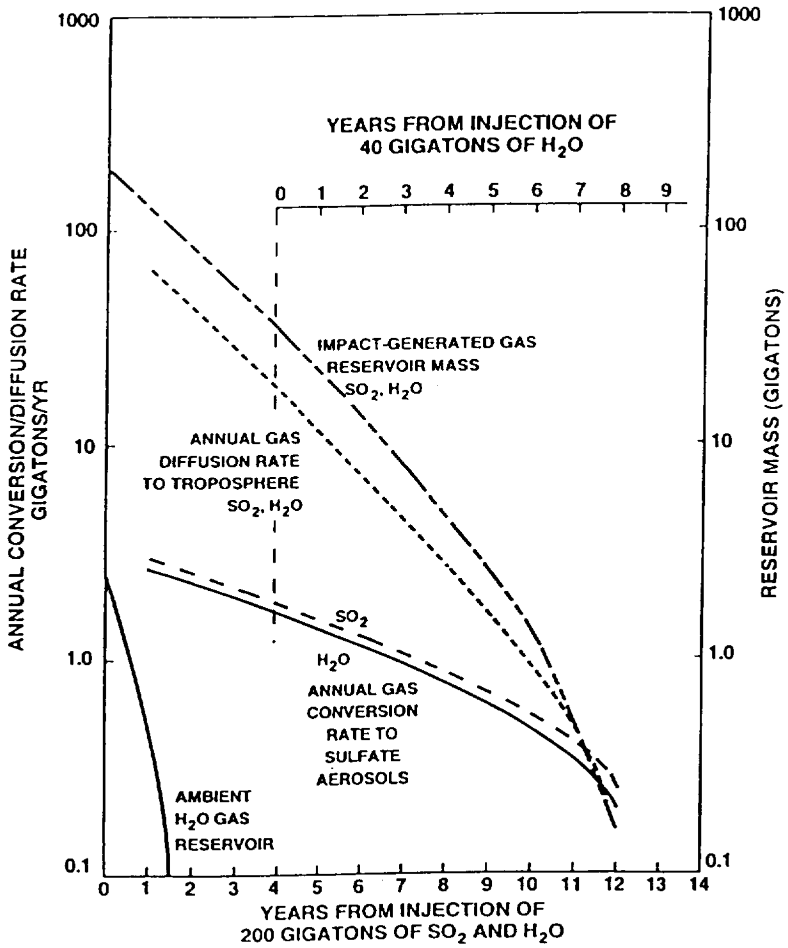

Figure 5. Evolution of the stratospheric SO_2 and H_2O impact-generated reservoirs. Reservoir masses (upper solid curve and righthand scale) are shown as a function of time for an initial loading of 200 Gt each of SO_2 and H_2O (for simplicity the SO_2/H_2O mass ratio for aerosol formation is shown as 1, actual ratios are 1.02-1.19). The upper horizontal scale gives a similar time line for a loading of 40 Gt each of SO_2 and H_2O. The upper dashed curve and lefthand scale give the annual diffusion rates for SO_2 and H_2O. The lower solid and dashed curves and left hand scale give the annual rate of conversion of SO_2 and H_2O to sulfate aerosol. These curves demonstrate that diffusion is a much greater sink than conversion to aerosol until about the beginning of last year. For a 200 Gt loading, sulfate arosol production lasts about 12 years, and for a 40 Gt loading, about 8 years (note that aerosol loading will remain high for about one year after production ceases). The solid curve in the lower left shows the time required (~1.5 years) to deplete the ambient water reservoir with a 200 Gt loading of SO_2 without a similar injection of water, emphasizing the importance of injections of both water and SO_2 in the process.

(ignoring absorptions by soot and dust as well as by enhanced SO_2, H_2O, and CO_2 reservoirs). Such an 80% reduction would have cooled the surface tremendously, but not greatly effect photosynthesis. Thermal emission from sulfate particles mitigates the ground surface cooling somewhat, however the area-weighted mean radius of the sulfate particles is $\leq$0.85 microns, well within the net cooling regime of Lacis et al. (1992). Near the bottom of the stratosphere, the older aerosols reach a mean particle size greater than 2.0 microns, indicating that these particles contribute no net cooling, but perhaps a net warming (Lacis et al., 1992). Nevertheless, these aerosols contribute less than 10% of the net cross-section to sunlight, thus the predominant effect of the impact-generated sulfate aerosols is to severely cool the Earth's surface.

Figure 6 shows the transmission of sunlight to the Earth's surface (relative to pre-impact conditions) as a function of time for three impact-generated SO_2-H_2O reservoirs of 20, 200, and 2,000 Gt each, which bracket the minimum and maximum possible values noted above (SO_2: 100-1000 Gt and H_2O: 30-1700 Gt). Stratospheric sulfate aerosols decrease the transmission by about ~80-90% in the year following the impact, and remains more than 20% below normal for ~12 years for the 200 Gt case, ~7 years for the 20 Gt case, and ~18 years for the 2,000 Gt case.

Impact Induced Climate Change at the K/T Boundary

The annual average reduction in solar transmission over 12 years predicted for our nominal 200 Gt case is 68%, which represents an average climate forcing of about -160

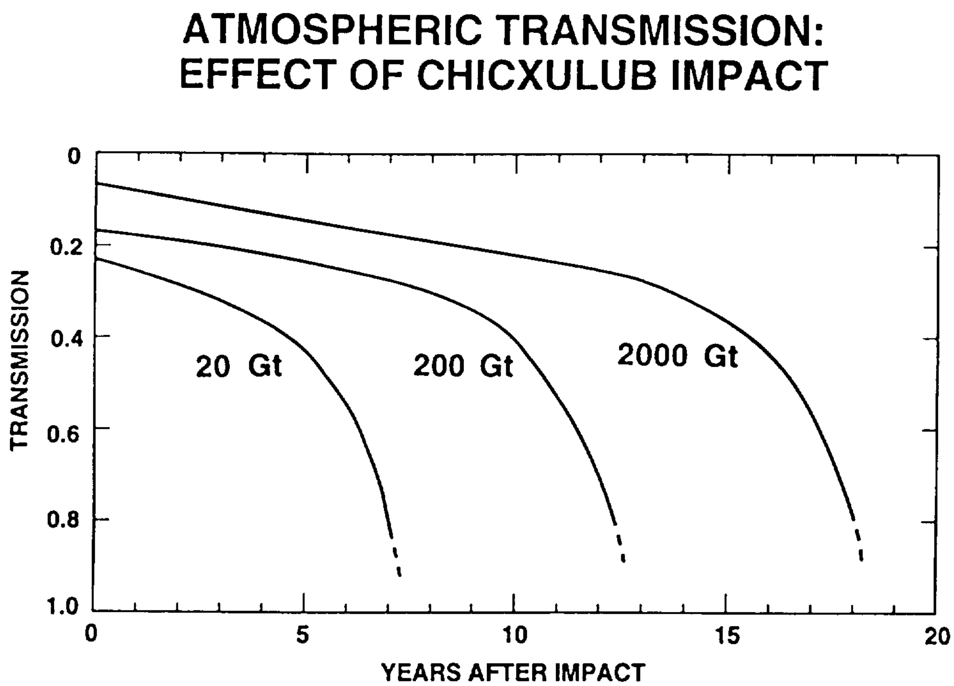

Figure 6. Atmospheric transmission (0.5 microns) following the Chicxulub impact. Post-impact transmission, relative to pre-impact, is shown as a function of time for three cases: 20 Gt, 200 Gt, and 2,000 Gt loadings of SO_2. Transmission evaluated using the vertically-inhomogeneous aerosol model structure in Figure 3 and the stratospheric aerosol evolution shown in Figure 5.

W/m^2, corresponding to a -50°K cooling. Pollack et al. (1993) used a global climate model (GCM) to estimate the an e-fold time scale of 15 years for cooling by steady-state volcanic forcing. The GCM run included a coupled ocean-atmosphere regime, but only for the upper mixed layer of the ocean. Their model did not account for upwelling of deeper waters, which they suggest could increase the e-fold time to as much as 150 years. If we apply the 15 year time scale to the -50°C cooling of our nominal 200 Gt case, then over the 12 years the average surface temperature would have dropped 28°C. Today's average surface temperature is 15°C, and although the Late Cretaceous may have been slightly warmer, the application of the 15 year time scale predicts that temperatures may have dropped to freezing in about 5 years after the impact, followed by about 7 years of freezing or near-freezing conditions. Presumably another 5 years or more would be required for temperatures to return to normal.

Clearly the entire Earth did not freeze, which indicates that upwelling of deep waters must have played a role. If we apply the 150 year time scale, then temperatures would have dropped only about 4°C in 12 years. It is highly unlikely that deep ocean circulation would be this efficient over such a short time period with such high climate forcing, hence the 15 year time scale is probably more appropriate with moderate buffering from upwelling of deeper waters. We caution that temperature estimates such as these are very approximate, since there are a wide range of feedback mechanisms from such a large atmospheric perturbation as the Chicxulub impact. Nevertheless, these calculation demonstrate the potential for the Chicxulub impact to produce freezing conditions on a global scale.

Greenhouse warming from impact-generated CO_2 must also be considered. Our baseline estimates of 312-549 Gt of CO_2 are but a fraction of the 2,800 Gt ambient CO_2 content of today's atmosphere (Watson et al., 1990). About 600 Gt of CO_2 have been deposited in the atmosphere over the last 100 years by human activities, and many studies of this anthropogenic input of CO_2 have demonstrated that such low level inputs raised temperatures less than 1°C (e.g. Cubasch and Cess, 1990; Shine et al., 1990; Watson et al., 1990). Our maximum estimate of 1700 Gt of CO_2 would not even double today's levels. Models of such doubling of the CO_2 reservoir indicate a minor 1-2° C temperature increase (Cubasch and Cess, 1990). Therefore, greenhouse warming due to the impact release of CO_2 was negligible.

In summary, the vaporization of sulfates by the Chicxulub impact, and the subsequent generation of a long-lived sulfuric acid aerosol haze, caused major cooling during the decade after the impact. Within about 5 years after the impact surface temperatures may have dropped below freezing in many areas, especially continental regions. The upper mixed layer of the oceans cooled dramatically and widespread freezing was adverted only by upwelling of deep ocean waters. These factors played a major role in the mass extinction that marks the K/T boundary.

References

Alvarez, L.W., W. Alvarez, F. Asaro, and H.V. Michel, Extraterrestrial cause for the Cretaceous-Tertiary extinction, Science 208, 1095-1108, 1980.

Alvarez, W., and F. Asaro, An extraterrestrial impact, Scientific American 263, 78-84, 1990.

Alvarez, W., J. Smit, W. Lowrie, F. Asaro, S.V. Margolis, Ph. Claeys, M. Kastner, and A.R. Hildebrand, Proximal impact deposits at the Cretaceous-Tertiary boundaryin the Gulf of Mexico: A restudy of DSDP Leg 77 Sites 536 and 540: Geology 20, 697-700, 1992.

Alvarez, W., P. Claeys, and S. Kieffer, Emplacement of Cretaceous-Tertiary boundary shocked quartz from Chicxulub crater, Science 269, 930-935, 1995.

Badjukov, D.D., Dikov, Yu.P., T.L. Petrova, and S.V. Pershin, Shock behavior of calcite, anhydrite, and gypsum, Lunar Planet. Sci. XXVI, 63-64, 1995.

Baines, K.H., and W.H. Smith, The atmospheric structure and dynamical properties of Neptune derived from ground-based and IUE spectrophotometry, Icarus 85, 65-108, 1990.

Baines, K.H., and H.B. Hammel, Clouds, haze, and the stratospheric methane abundance in Neptune, Icarus 109, 20-39, 1994.

Boslough, M.B., T.J. Ahrens, J. Vizgirda, R.H. Becker, and S. Epstein, Shock-induced devolatilization of calcite, Earth Planet. Sci. Lett. 61, 166-170, 1982.

Brasseur, G., and C. Granier, Mount Pinatubo Aerosols, Chlorofluorocarbons, and ozone depletion, Science 257, 1239-1242.

Brett, R. The Cretaceous-Tertiary extinction: A lethal mechanism involving anhydrite target rocks, Geochim. et Cosmochim. Acta 56, 3603-3606, 1992.

Chaimberlain, J.W., Theory of Planetary Atmospheres: An Introduction to their Physics and Chemistry, New York, Academic Press, 1978.

Chen, G. and T.J. Ahrens, Shock-induced devolatilization of calcium sulfate and implications for K-T extinctions, Earth Planet. Sci. Lett. 128, 615-628, 1994.

Covey, C., S.J. Ghan, J.J. Walton, and P.R. Weissman, Global environmental effects of impact-generated aerosols: Results from a general circulation model, in Global Catastrophes in Earth History, edited by V.L. Sharpton and P.D. Ward, Boulder, Colorado, Geol. Soc. Amer. Spec. Pap. 247, 263-270, 1990.

Covey, C., S.L. Thompson, P.R. Weissman, and M.C. MacCracken, Global climatic effects of atmospheric dust from an asteroid or comet impact on Earth, Global and Planetary Change 9, 263-273, 1994.

Croft, S.K., The scaling of complex craters, J. Geophys. Res. 90, Supplement, C828-C842, 1985.

Cubasch, U., and R.D. Cess, Processes and modelling, in: Climate Change: The IPCC Scientific Assessment, J.T. Houghton, G.J. Jenkins, and J.J. Ephraums, eds., pp. 69-91, Cambridge U. Press, Cambridge, 1990.

Emiliani, C., E.B. Kraus, and E.M. Shoemaker, Sudden death at the end of the Mesozoic, Earth Planet. Sci. Lett. 55, 317-334.

Espindola, J.M., MN. Mena, M. de La Fuente, and J.O. Campos-Enriquez, A model of the Chicxulub impact structure (YUcatan, Mexico) based on its gravity and magnetic signatures, Phys. Earth Planet. Interiors 92, 271-278, 1995.

Gerasimov, M.V., Y.P. Dikov, O.I. Yakovlev, and F. Wlotzka, High-temperature vaporization of gypsum and anhydrite: Experimental results, Lunar Planet. Sci. XXV, 413-414, 1994.

Gerasimov, M.V., Y.P. Dikov, O.I. Yakovlev, and F. Wlotzka, High-temperature vaporization of quartz-calcit-anhydrite/gypsum targets in relation to Chicxulub impact, Lunar Planet. Sci. XXVI, 451-452, 1995.

Gerstl, S.A.W., and A. Zardecki, Reduction of photosynthetically active radiation under extreme stratospheric aerosol loads, Geol. Soc. Amer. Spec. Paper 190, 201-210, 1982.

Grieve, R.A.F., P.B. Robertson, and M.R. Dence, Constraints on the formation of ring impact structures, based on terrestrial data, in Proceedings of the Conference on Multi-ring Basins: Formation and Evolution, edited by R.B. Merrill and P.H. Schultz, pp. 37-57, New York, Pergamon, 1981.

Haq, B.U., J. Hardenbol, and P.R. Vail, Chronlogyyy for fluctuating sea level since the Triassic, Science 235, 1156-1166, 1987.

Hansen, J.E., and J.W. Hovenier, Interpretation of the polarization of Venus, J. Atmos. Sci. 31, 1137-1160, 1974.

Hildebrand, A.R., G.T. Penfield, D.A. Kring, M. Pilkington, A. Camargo Z., S.B. Jacobnsen, and W.V. Boynton, Chicxulub crater: A possible Cretaceous/Tertiary boundary impact crater on the Yucatan Peninsula, Mexico, Geology 19, 867-871, 1991.

Hildebrand, A. R., and J.A. Stansberry, K/T boundary ejecta distribution predicts size and location of Chicxulub crater, Lunar Planet. Sci. XXIII, 537-538, 1992.

Hildebrand, A. R., Connors, M., Pilkington, M., Ortiz Aleman, C., and Chavez, R. E., Size and structure of the Chicxulub crater: Sociedad Mexicana de Paleontologia Revista 7, 59-68, 1994.

Hildebrand, A.R., Pilkington, M., Connors, M., Ortiz-Aleman, C., and Chavez, R.E., 1995. Size and structure of the Chicxulub crater revealed by horizontal gravity gradients and cenotes: Nature, v. 376, p. 415-417.

Holton, J.R., On the global exchange of mass between the stratosphere and troposphere, J. Atmos. Sci. 47, 392-395, 1990.

Houghton, J.T., The Physics of Atmospheres. New York, Cambridge University Press, 1977.

Ivanov, B.A., D.D. Badukov, O.I. Yakovlev, M.V. Gerasimov, Yu.P. Dikov, K.O. Pope, and A.C. Ocampo, Degassing of Sedimentary rocks due to Chicxulub impact: Hydrocode and Physical Simulations, in The Cretaceous-Tertiary Event and Other Catastrophes in Earth History, edited by G. Ryder, D. Fastovsky, and S. Gartner, Boulder, Colorado, Geol. Soc. Amer. Spec. Paper, in press.

Jablonsky, D., Mass extinctions: Persistent problems and new directions, in New Developments Regarding the KT Event and Other Catastrophes in Earth History, LPI Contribution 825, 56-57, 1994.

Keller, G., N. MacLeod, J.B. Lyons, and C.B. Officer, Is there evidence for Cretaceous-Tertiary boundary-age deep-water deposits in the Caribbean and Gulf of Mexico? Geology 21, 776-780.

Kieffer, S.W., and C.H. Simonds, The role of volatiles and lithology in the impact craterin process, Rev. Geophys. Space Phys. 18, 143-181, 1980.

Krasnopolsky, V.A., and V.A. Parshev, Photochemistry of the Venus atmosphere, in Venus, edited by D.M. Hunten. L. Colin, T.M. Donahue, and V.I. Moroz, pp. 431-458, Tucson, University of Arizona Press, 1983.

Kring, D. A., 1995, The dimensions of the Chicxulub crater and impact melt sheet: Journal of Geophysical Research, v. 100, p. 16,979-16,986.

Kyte, F.T., J. Smit, and J.T. Wasson, Siderophile interelement variations in the Cretaceous-Tertiary boundary sediments from Caravaca, Spain, Earth Planet. Sci. Lett. 73, 183-195, 1985.

Labitzke, K., B. Naujokat, and M.P. McCormick, Temperature effects on the stratosphere of the April 4, 1982 eruption of El Chichon, Mexico, Geophys. Res. Lett. 10, 24-26, 1983.

Lacis, A., J. Hansen, and M. Sato, Climate forcing by stratospheric aerosols, Geophys. Res. Lett. 19, 1607-1610, 1992.

Lang, M.A., and T.J. Ahrens, Shock-induced CO_2 loss from Ca CO_3; implications for early planetary atmospheres, Earth Planet. Sci. Lett. 77, 409-418, 1986.

Lopez Ramos, E. Geologia de Mexico, Tomo III, 445 pp., Mexico, 1979.

Lyons, J.R., and T.J. Ahrens, Chicxulub impact-induced vaporization: S and C species and their affect on global climate, Lunar Planet. Sci. XXVII, 787-788, 1996.

Margitan, J.J., Mechanics of the atmospheric oxidation of sulfur dioxide. Catalysis of hydroxyl radicals, J. Phys. Chem. 88, 3314-3318, 1984.

Martinez, I., P. Agrinier, U. Scharer, and M. Javoy, A SEM-ATEM and stable isotope study of carbonates from Haughton impact crater, Canada, Earth Planet. Sci. Lett. 121, 559-574, 1994.

Martinez, I., A. Deutsch, U. Scharer, P. Idefonse, F. Guyot, and P. Agrinier, Shock recovery experiments on dolomite and thermodynamical calculations of impact induced decarbonation, J. Geophys. Res. 100, 15,465-15,476, 1995.

McGetchin, T.R., M. Settle, and J.W. Head, Radial thickness variation in impact crater ejecta: Implications for lunar basin deposits, Earth Planet. Sci. Lett. 20, 226-236, 1973.

Melosh, H.J., 1989, Impact Cratering: A Geologic Process: New York, Oxford University Press, 245 pp.

Ocampo, A.C., K.O. Pope, and A.G. Fischer, Ejecta blanket deposits of the Chicxulub crater from Albion Island, Belize, in The Cretaceous-Tertiary Event and Other Catastrophes in Earth History, edited by G. Ryder, D. Fastovsky, and S. Gartner, Boulder, Colorado, Geol. Soc. Amer. Spec. Paper, in press.

O'Keefe, J.D., and T.J. Ahrens, Impact production of CO_2 by the K/T extinction bolide and the resultant heating of the Earth, Nature 338, 247-249, 1989.

Palmer, K.F., and D. Williams, Optical constants of sulfuric acid, Appl. Optics 14, 208-219, 1975.

Pierazzo, E., H.J. Melosh, and D.A. Kring, Numerical simulation of the Chicxulub impact event, Lunar Planet. Sci. XXVII, 1029-1030.

Pilkington, M., A.R. Hildebrand, and C. Ortiz-Aleman, Gravity and magnetic field modeling and structure of the Chicxulub crater, Mexico, J. Geophys. Res. 99, 13,147-13,162, 1994.

Pinto, J.P, R.P. Turco, and O.B. Toon, Self-limiting physical and chemical effects in volcanic eruption clouds, J. Geophys. Res. 94, 11,165-11,174, 1989.

Poag, C.W., Structural outer rim of Chesapeake Bay impact crater: Siesmic and bore hole evidence, Meteor. Planet. Sci. 31, 218-226, 1996.

Pollack, J.B., O.B. Toon, T.P. Ackerman, C.P. McKay, and R.P. Turco, Environmental effects of an impact-generated dust cloud: implications for the Cretaceous-Tertiary extinctions, Science 219, 287-289, 1983.

Pollack, J.B., D. Rind, A. Lacis, J.E. hansen, M. Sato, and R. Ruedy, GCM simulations of volcanic aerosol forcing. Part I: Climate changes induced by steady-state perturbations, J. Climate 6, 1719-1742, 1993.

Pope, K.O., A.C. Ocampo, and C.E. Duller, Mexican site for K/T impact crater?, Nature 351, 105, 1991.

Pope, K.O., A.C. Ocampo, and C.E. Duller, Surficial geology of the Chicxulub impact crater, Yucatan, Mexico, Earth Moon Planets 63, 93-104, 1993.

Pope, K.O., K.H. Baines, A.C. Ocampo, and B.A. Ivanov, Impact winter and the Cretaceous/Tertiary extinctions: Results of a Chicxulub asteroid impact model, Earth and Planetary Science Letters 128, 719-725, 1994.

Pope, K.O., A.C. Ocampo, G.L. Kinsland, and R. Smith, Surface expression of the Chicxulub crater, Geology, in press.

Rabinowitz, D., E. Bowell, E. Shoemaker, and K. Muinonen, The population of Earth-crossing asteroids, in Hazards Due to Comets and Asteroids, edited by T. Gehrels, pp. 285-312, Tucson, University of Arizona Press, 1994.

Rampino, M.R., and S. Self, Volcanic winter and accelerated glaciation following the Toba super-eruption, Nature 359, 50-52, 1992.

Raup, D.M., and J.J. Sepkoski Jr. Mass extinctions in the marine fossil record, Science 215, 1501-1503, 1982.

Raup, D.M., and J.J. Sepkoski Jr. Periodic extinctions of families and genera, Science 231, 833-836, 1986.

Rose, W.I., and C.A. Chesner, Worldwide dispersal of ash and gases from earth's largest known eruption: Toba, Sumatra, 75 ka, Palaeogeogr. Palaeoclim. Palaeoecol. 89, 269-

275, 1990.

Schmidt, R.M., and K.R. Housen, Some recent advances in the scaling of impact and explosion cratering, Int. J. Impact Engin. 5, 543-560, 1987.

Schultz, P.H., Visualizing the nature and consequences of the Chicxulub impactor: Clues from Venus, in New Developments Regarding the KT Event and Other Catastrophes in Earth History, LPI Contribution 825, 104-106, 1994.

Schultz, P.H., Chicxulub impact angle and consequences, Geol. Soc. Amer. Abstr. Program., pp. A349, New Orleans, 1995.

Schultz, P.H., and D.E. Gault, Prolonged global catastropphes from oblique impacts, in Global Catastrophes in Earth History, edited by V.L. Sharpton and P.D. Ward, Boulder, Colorado, Geol. Soc. Amer. Spec. Pap. 247, 239-261, 1990.

Sepkoski Jr., J.J. The taxonomic structure of periodic extinction, Geol. Soc. Amer. Spec. Paper 247, 33-44, 1990.

Sharpton, V.L., G.B. Dalrymple, L.E. Marin, G. Ryder, B.C. Schuraytz, and J. Urrutia-Fucugauchi, New links between the Chicxulub impact structure and the Cretaceous/Tertiary boundary, Nature, 359, 819-821, 1992.

Sharpton, V.L., K. Burke, A. Camargo-Zanoguera, S.A. Hall, D.S. Lee, L.E. Marin, G. Suarez-Reynoso, J.M. Quezada-Muneton, P.D. Spudis, and J. Urrutia-Fucugauchi, Chicxulub multiring impact basin: Size and other characteristics derived from gravity analysis, Science 261, 1564-1567, 1993.

Sharpton, V.L., L.E. Marin, J.L. Carney, S. Lee, G. Ryder, B.C. Schuraytz, P. Sikora, and P.D. Spudis, A model of the Chicxulub impact basin based on evaluation of geophysical data, well logs and drill core samples, in The Cretaceous-Tertiary Event and Other Catastrophes in Earth History, edited by G. Ryder, D. Fastovsky, and S. Gartner, Boulder, Colorado, Geol. Soc. Amer. Spec. Paper, in press.

Shine, K.P., R.G. Derwent, D.J. Wuebbles, and J.-J. Morcrette, Radiative forcing of climate, in: Climate Change: The IPCC Scientific Assessment, J.T. Houghton, G.J. Jenkins, and J.J. Ephraums, eds., pp. 41-68, Cambridge U. Press, Cambridge, 1990.

Shoemaker, E.M., R.F. Wolfe, and C.S. Shoemaker, Asteroid and comet flux in the neighborhood of Earth, in Global Catastrophes in Earth History, edited by V.L. Sharpton and P.D. Ward, Boulder, Colorado, Geol. Soc. Amer. Spec. Pap. 247, 155-170, 1990.

Sigurdsson, H., Ph. Bonte, L. Turpin, M. Chaussidon, N. Metrich, M. Steinberg, Ph. Pradel and S. D'Hondt, Geochemical constraints on source region of Cretaceous/Tertiary impact glasses, Nature, 353, 839-842, 1991.

Sigurdsson, H., S. D'Hondt, and S. Carey, The impact of the Cretaceous/Tertiary bolide on evaporite terrain and the generation of major sulfuric acid aerosol, Earth Planet. Sci. Lett. 109, 543-559, 1992.

Smit, J., A. Montanari,N.H.M. Swinburne, W. Alvarez, A. Hildebrand, S.V. Margolis, P. Claeys, W. Lowrie, and F. Asaro, Tektite bearing deep-water clastic unit at the Cretaceous-Tertiary boundary in northeastern Mexico, Geology 20, 99-103, 1992.

Smit, J., Th.B. Roep, W. Alvarez, Ph. Claeys, and A. Montanari, Comment on Stinnesbeck et al. 1993 and Keller et al 1993, Geology 22, 953-954, 1994.

Sohl, N.F., E. Martinez R., P. Salmeron-Urena, and F. Soto-Jaramillo, Upper Cretaceous, in The Geology of the Gulf of Mexico Basin, edited by A. Salvador, pp. 205-244, Boulder, Colorado, Geol. Soc. Amer., The Geology of North America, vol. J.

Sinnesbeck, W., J.M. Barbarin, G. Keller, J.G. Lopez-Oliva, D.A. Pivnik, J.B. Lyons, C.B. Officer, T. Adatte, G. Graup, R. Rocchia, and E. Robin, Deposition of channel deposits near the Cretaceous-Tertiary boundary in northeastern Mexico: Catastrophic or "normal" sedimentary deposits? Geology 21, 797-800, 1993.

Sinnesbeck, W., G. Keller, T. Adatte, and N. MacLeod, Reply to Smit et al. 1994, Geology 22, 955-956, 1994.

Swisher, III, C.C., J.M. Grajales-Nishimura, A. Montsanari, S.V. Margolis, P. Clayes, W. Alvarez, P. Renne, E. Cedillo-Pardo, F.J.-M.R. Maurrassee, G.H. Curtis, J. Smit, and M.O. McWilliams, Coeval $^{40}Ar/^{39}Ar$ ages of 65.0 million years ago for Chicxulub crater melt rock and Cretaceous-Tertiary boundary tektites, Science 257, 954-958, 1992.

Takata, T., and T.J. Ahrens, Physical properties of comet Shoemaker-Levy 9: Origin and progenitor size, Lunar Planet. Sci. XXVI, 1391-1392, 1995.

Toon, O.B., J.B. Pollack, T.P. Ackerman, R.P. Turco, C.P. McKay, and M.S. Liu, Evolution of an impact-generated dust cloud and its effects on the atmosphere, Geol. Soc. Amer. Spec. Paper 190, 187-200, 1982.

Toon, O.B., Zahnle, K., Turco, R.P., and Covey, C., Environmental perturbations caused by asteroid impacts, in Hazards Due to Comets and Asteroids, edited by T. Gehrels, pp. 791-826, Tucson, University of Arizona Press, 1994.

Tyburczy, J.A., and T.J. Ahrens, Dynamic compression and volatile release of carbonates, J. Geophys. Res. 91, 4730-4744, 1986

Watson, R.T., H. Rodhe, H. Oeschger, and U. Siegenthaler, Greenhouse gases and aerosols, in: Climate Change: The IPCC Scientific Assessment, J.T. Houghton, G.J. Jenkins, and J.J. Ephraums, eds., pp. 1-40, Cambridge U. Press, Cambridge, 1990.

Ward, W.C., G. Keller, W. Stinnesbeck, and T. Adatte, Yucatan subsurface stratigraphy: Implications and constraints for the Chicxulub impact, Geology 23, 873-876, 1995.

Vickery, A.M., and H.J. Melosh, Atmospheric erosion and impactor retension in large impacts, with application to mass extinction, in Global Catastrophes in Earth History, edited by V.L. Sharpton and P.D. Ward, Boulder, Colorado, Geol. Soc. Amer. Spec. Pap. 247, 289-300, 1990.

Vickery, A.M., D.A. Kring, and H.J. Melosh, Ejecta associated with large terrestrial impacts: Implications for the Chicxulub impact and K/T boundary stratigraphy, Lunar Planet. Sci. XXIII, 1473-1474, 1992.

Viniegra-O., F., Great Carbonate Bank of Yucatan, southern Mexico, J. Petrol. Geol. 3, 247-278, 1981.

Weidie, A.E. Geology of Yucatan platform, in: Geology and Hydrology of the Yucatan and Quaternary Geology of Northeastern Yucatan Peninsula, W.C. Ward, A.E. Weidie, and W. Back, eds., pp. 1-19, New Orleans Geological Society, New Orleans, 1985.

Yang, W., T.J. Ahrens, and G. Chen, Shock vaporization of anhydrite and calcite and the effects on global climate from the K/T impact crater at Chicxulub, Lunar Planet. Sci. XXVII, 1473-1474, 1996.

Zahnle, K., M.-M. MacLow, K.Lodders, and B. Fegley, Jr., Sulfur chemistry in the wake of comet Shoemaker-Levy 9, Geophys. Res. Lett. 22, 1593-1596, 1995.

Zahnle, K.J., Atmospheric chemistry by large impacts, in Global Catastrophes in Earth History, edited by V.L. Sharpton and P.D. Ward, Boulder, Colorado, Geol. Soc. Amer. Spec. Pap. 247, 271-288, 1990.

Zielinski, G.A., P.A. Mayewski, L.D. Meeker, S. Whitlow, M.S., Twickler, and K. Taylor, Potential atmospheric impact of the Toba mega-eruption ~71,000 years ago, Geophys. Res. Lett. 23, 837-840.

REPORT DOCUMENTATION PAGE

Form Approved
OMB No. 0704-0188

1. AGENCY USE ONLY (Leave blank)

2. REPORT DATE
6/14/96

3. REPORT TYPE AND DATES COVERED
5/15/93 - 6/14/96 Final Report

4. TITLE AND SUBTITLE
Biospheric Effects of Volatiles Produced by the Chicxulub Cretaceous/Tertiary Impact

5. FUNDING NUMBERS
NASW-4812

6. AUTHOR(S)
Kevin O. Pope

7. PERFORMING ORGANIZATION NAME(S) AND ADDRESS(ES)
Geo Eco Arc Research
2222 Foothill Blvd. Suite E-272
La Cañada, CA 91011 USA

8. PERFORMING ORGANIZATION REPORT NUMBER

9. SPONSORING/MONITORING AGENCY NAME(S) AND ADDRESS(ES)
NASA Exobiology Program

10. SPONSORING/MONITORING AGENCY REPORT NUMBER
Code SR
NASA Headquarters

11. SUPPLEMENTARY NOTES

12a. DISTRIBUTION/AVAILABILITY STATEMENT
No restrictions

12b. DISTRIBUTION CODE
No limitations

13. ABSTRACT (Maximum 200 words)

The meteorite impact that formed the Chicxulub crater 65 million years ago caused a mass extinction of life. Analyses indicate that the projectile was either a 9.4-16.8 km diameter asteroid or a 14.2-24.0 km diameter comet. We estimate that 200 gigatons each of SO_2 and H_2O were deposited globally in the stratosphere by the impact into water saturated sulfate-rich sediments. Conversion of these gases into sulfuric acid aerosols blocked an average of 68% of the sun's radiation for a period of 12 years. Global average temperatures probably dropped to near freezing in 5 years and remained near or below freezing for 7 years. Greenhouse warming due to impact-generated CO_2 was negligible, hence global cooling from sulfates was the major cause of climate change and contributed greatly to the mass extinction.

14. SUBJECT TERMS
Impact, Craters, Exobiology, Mass Extinction

15. NUMBER OF PAGES

16. PRICE CODE

17. SECURITY CLASSIFICATION OF REPORT
Non-Classified

18. SECURITY CLASSIFICATION OF THIS PAGE
None

19. SECURITY CLASSIFICATION OF ABSTRACT
None

20. LIMITATION OF ABSTRACT
None

NSN 7540-01-280-5500

Standard Form 298 (Rev. 2-89)
Prescribed by ANSI Std. Z39-18
298-102